Eur Biophys J (1990) 18:139–148

European Biophysics Journal

Primary sequence dependence of conformation in oligomannose oligosaccharides

E. W. Wooten, R. Bazzo, C. J. Edge, S. Zamze, R. A. Dwek, and T. W. Rademacher

Oxford Glycobiology Unit, University of Oxford, Oxford OX1 3QU, United Kingdom

Received August 8, 1989/Accepted in revised form December 2, 1989

Abstract. The oligomannose series of oligosaccharides from bovine thyroglobulin (BTG) and the variant surface glycoprotein (VSG) of *Trypanosoma brucei* have been isolated and sequenced by ^{1}H NMR. The structure of $Man_9GlcNAc_2$, the parent molecule of the series, is shown below. Structural isomerism occurs within this series through the removal of residues D1, D2, D3, and C. Using spin-spin coupling and chemical shift data the rotamer distributions about the dihedral angle ω for the Manα1–6Manβ and Manα1–6Manα linkages were determined for each member of the series. It is shown that the dihedral angle ω of the Manα1–6Manβ linkage exhibits low flexibility with a preference for the $\omega = 180°$ conformation when residue D2 is present and high flexibility when this residue is absent. Flexibility of ω for the Manα1–6Manα is largely independent of primary sequence and is intermediate between the two Manα1–6Manβ extremes, again with a preference for the $\omega = 180°$ conformation.

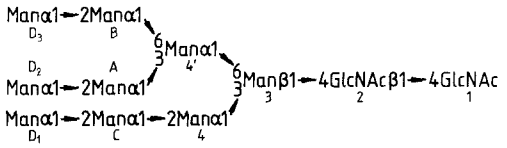

There are, however, data which indicate that removal of residue D3 may confer additional flexibility upon the dihedral angle ω of the Manα1–6Manα linkage. Molecular graphics modelling, together with chemical and enzymatic modification studies, suggest that the origin of the observed primary sequence dependence of the Manα1–6Manβ linkage arises from steric factors. On the basis of these observations taken together with previous work, it is postulated that recognition of individual oligomannose conformations may play a role in the control of N-linked oligosaccharide biosynthesis.

Key words: NMR – Conformation – Oligosaccharides

Introduction

Oligosaccharides have been implicated in a wide range of biological phenomena and are thought to play important biological roles, in both health and disease states (Rademacher et al. 1988). An attempt to rationalise these phenomena on a molecular level requires a knowledge of the three dimensional structure of oligosaccharides. ^{1}H NMR is at present the most precise method of determining oligosaccharide solution structure, and many studies of oligosaccharide solution conformation have been performed (Bock et al. 1982; Brisson and Carver 1983b, c; Paulsen et al. 1986; Homans et al. 1983b; Homans et al. 1987a–c; Koerner et al. 1987).

The picture which has gradually emerged is that oligosaccharides have definite secondary structure which is in some way dependent upon primary sequence. Furthermore, solution conformations of oligosaccharides often exhibit regions of both ordered and disordered structure (Homans et al. 1987b). The flexibility of 1–6 linkages is not surprising since for linkages other than the 1–6, the two rigid sugar rings are separated by a single atom, whereas two atoms separate the rings in the 1–6 case. As a consequence, the motion about the torsional angles ϕ = H1C1O1CX and ψ = C1O1CXHX of this glycosidic linkage will be intrinsically less hindered. An additional feature of 1–6 linkages is that there can be free rotation about a further bond, so that in addition to torsional angles ϕ and ψ, the dihedral angle ω = O6C6C5H5 must also be characterised. These angles are shown in Fig. 1.

Abbreviations: AMBER, assisted model building with energy refinement; BTG, bovine thyroglobulin; COSY, ^{1}H-^{1}H correlation spectroscopy; Endo-H, endo-β-N-acetylglucosaminidase H; NMR, nuclear magnetic resonance; NOE, nuclear Overhauser effect; NOESY, two dimensional ^{1}H-^{1}H nuclear Overhauser effect spectroscopy; HOHAHA, homonuclear Hartmann-Hahn spectroscopy; HSEA, hard sphere exo-anomeric effect, RECSY, multistep relayed correlation spectroscopy; VSG, variant surface glycoprotein

Offprint requests to: T. W. Rademacher

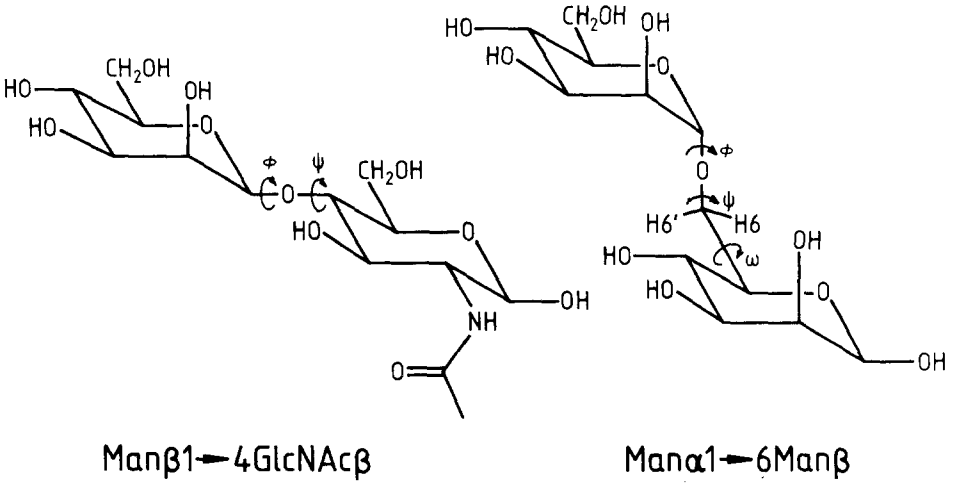

Fig. 1. The disaccharides Manβ1–4GlcNAcβ and Manα1–6Manβ showing the dihedral angles ϕ, ψ, and ω

The angle ω is extremely important since changes in this angle will drastically alter the overall three dimensional appearance of an oligosaccharide, whereas the same may not be true for transitions of ϕ and ψ. Hence, a good deal of literature can be found involving the determination of ω in oligosaccharides and model compounds using chemical shift, spin coupling, and theoretical data (Marchessault and Perez 1979; Bock et al. 1982; Brisson and Carver 1983a, c; Paulsen et al. 1986; Homans et al. 1986; Berman 1987; Cumming and Carver 1987; Biswas et al. 1987; Nishida et al. 1988). We have previously examined rotamer distributions about ω (Homans et al. 1986) in the oligomannose oligosaccharides $Man_9GlcNAc_2$ and $Man_5GlcNAc_2$, the beginning and ending structures of a section of the N-linked oligosaccharide biosynthetic pathway. It was found (Homans et al. 1986) that in $Man_9GlcNAc_2$, both 1–6 linkages are restricted to a single value of ω, whereas the same linkages oscillate between two equally populated conformers in $Man_5GlcNAc_2$. In order to determine the reason why the two very similar structures have such different conformational properties, it is necessary to look at a series of structurally related compounds.

In this study, the major naturally occurring oligomannose biosynthetic intermediates $Man_9GlcNAc_2$–$Man_5GlcNAc_2$ from bovine thyroglobulin and the variant surface glycoprotein of *T. brucei* are isolated and sequenced using ^{1}H NMR. Sequence specific assignment enables $J_{5\,6}$ and $J_{5\,6'}$ to be measured and the distribution of rotamers about both α1–6 linkages to be calculated for each compound. Because we examine a series consisting of isomers, we are able to relate specific changes in oligosaccharide primary sequence to specific changes in secondary structure, and can therefore generate "selection rules" for conformational transitions in oligomannose oligosaccharides. We find in particular that the rotamer distributions are primary sequence dependent, with major variation associated with the Manα1–6Manβ linkage, and that this primary sequence dependence can be traced to the presence or absence of mannoses D2 and D3. Molecular modelling together with chemical and enzymatic modification studies provide some insight into the physical basis for the observed rules, the significance of which are discussed in light of current theories of oligosaccharide biosynthesis.

Experimental procedures

Preparation of oligomannose oligosaccharides

Oligomannose oligosaccharides were isolated from bovine thyroglobulin (BTG) and the variant surface glycoprotein (VSG) of *T. brucei* using methods similar to those previously described (Homans et al. 1984; Ashford et al. 1987; Parekh et al. 1987; Zamze et al. 1989). The intact, unreduced sugars were purified using gel filtration chromatography with refractive index detection.

2 mg of $Man_9GlcNAc_2$ was reduced with sodium borodeuteride in 100 m*M* NaOH/boric acid buffer (0.25 *M* $NaBH_4$ in 0.5 ml, 4 h, 25 °C, pH 11.0). Deionisation was accomplished by passing the sample down a column of A650 × 12(H^+) after acidifying with glacial acetic acid. The borate was removed by flash evaporation with methanol, and finally a few drops of toluene were added and flash evaporated. Reduction was seen to be complete by ^{1}H NMR. 1 mg of $Man_9GlcNAc_2$OD was incubated with endo-β-N-acetylglucosaminidase H (Endo H, *Streptomyces plicatus*, Boehringer – Mannheim) at 20 units/ml in 200 µl of 100 m*M* citrate buffer (pH 5.4, 37 °C, 17 h under toluene). The reaction was stopped by heating at 100 °C for 2 min. Purification by ion exchange chromatography and filtration were performed as before. Gel filtration with refractive index detection together with ^{1}H NMR showed digestion to be complete. $Man_9GlcNAc$ was reduced and purified as above.

NMR Spectroscopy

Samples for ^{1}H NMR were prepared as previously described (Homans et al. 1984). Concentrations varied between 5 m*M* and <0.2 m*M*. One dimensional ^{1}H NMR spectra were obtained at 500 MHz on a Bruker AM500 at

a probe temperature of 300 K. A sweep width of 1200 Hz and 8192 time domain points were used with a recycle time of 5 s. All chemical shifts are relative to DSS (indirectly to acetone, $\delta = 2.225$ ppm).

Two dimensional ^{1}H-^{1}H COSY experiments (Aue et al. 1976; Marion and Wuthrich 1983; Homans et al. 1983a) were performed using 64 signal-averaged transients consisting of 2048 total points in t_2, 512 points in t_1, and a recycle time of 1 s. The time domain data were zero-filled in t_1 to 2048 total points and multiplied by unshifted sine-bell functions in both dimensions prior to transformation.

Phase sensitive NOESY spectra (Jeener et al. 1979; Kumar et al. 1980; Macura et al. 1981; Homans et al. 1983b) were recorded under identical conditions to those in COSY, except using 128 scans per t_1 and Gaussian multiplication for resolution enhancement. A mixing time of 500 ms was used. For precise measurement of $J_{5\,6}$ and $J_{5\,6'}$ in $Man_9GlcNAc_2$ and $Man_5GlcNAc_2$, 4096 points were collected in t_2 to improve digital resolution. After transformation in both dimensions, the relevant row for measuring J was selected, inverse Fourier transformed, multiplied by an unshifted sine-bell to minimise line-overlap errors, and zero-filled to 8192 points. The resulting FID was then transformed to give a spectrum from which J was measured.

A phase sensitive (TPPI) version of the RECSY experiment with incremented delays (Eich et al. 1982; Homans et al. 1984) was performed under the same conditions as in COSY except using 164 scans per t_1. Zero-filling and multiplication with unshifted sine-bell functions in both dimensions produced a 2-D map with minimal dispersion tails. HOHAHA experiments were performed as previously described (Homans et al. 1987d).

Computer graphics structures were generated as described previously (Homans et al. 1987c; Homans et al. 1989).

Results

The oligomannose oligosaccharides from BTG and VSG were assigned and sequenced using the methods described previously (Vliegenthart et al. 1983; Homans et al. 1986; Homans et al. 1987b). In particular, the assignment of the resonance positions of the chemically equivalent H6 protons is based on the work of Homans et al. Because of structural isomerism, confusion can arise over whether minor components come from cross-contamination with adjacent chromatography peaks or whether they are true minor isomers. We find that the 4H1/4H2 cross-peak position in COSY is a sensitive probe of primary sequence. Consideration of the entire oligomannose series allows specific cross-peak positions to be assigned to specific structures and resolves all ambiguity except for one case. It is not possible to say whether the small cross-peak in the COSY of $Man_7GlcNAc_2$ from BTG is M7 (D2) or contaminating M8 (D2, D3) and so M7 (D2) is not included in the study. Table 1 lists the major oligomannose oligosaccharides of BTG and VSG.

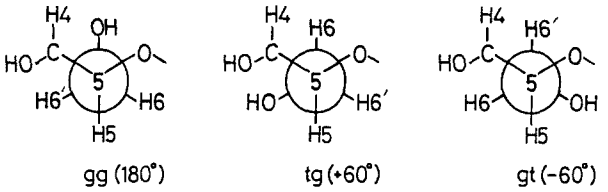

Fig. 2. The conformation about the C5-C6 bond is defined by the dihedral angle $\omega = O6C6C5H5$. Values of ω are given in parentheses for the gauche-gauche (gg), trans-gauche (tg), and gauche-trans (gt) rotamers

The dihedral angle ω is defined as O6C6C5H5 with positive values of ω corresponding to anticlockwise rotations of C5H5 while looking down the C5C6 bond as shown in Fig. 2. The Karplus equation (Karplus 1959), modified and applied to carbohydrates (Altona and Haasnoot 1980; Haasnoot et al. 1980; Wu et al. 1983; Nishida et al. 1988), gives a fairly accurate relationship for calculating J's from dihedral angle. The observed J will then be an average obtained from the sums of products:

$$J_{5\,6}(\text{obs}) = J_{5\,6}(60)\,P_{60} + J_{5\,6}(180)\,P_{180} + J_{5\,6}(-60)\,P_{-60}$$

$$J_{5\,6'}(\text{obs}) = J_{5\,6'}(60)\,P_{60} + J_{5\,6'}(180)\,P_{180} + J_{5\,6'}(-60)\,P_{-60}$$

$$1 = P_{60} + P_{180} + P_{-60}\,,$$

assuming fast rotation on the NMR timescale and the three state model of Fig. 2.

NOESY can resolve the H6 and H6′ protons of residues 3 and 4′ and can in principle give two measurements for each J. There is an NOE from 4′H1 to 3H6 and 3H6′ and from BH1 to 4′H6 and 4′H6′; plus, the H6/H6′ correlations can be observed for residues 3 and 4′. It is desirable to measure the J's from the H6/H6′ correlation since the signal-to-noise ratio of these peaks is greater than for the H1 to H6 and H6′ connectivities. Provided that care is taken to ensure that contributions from line overlap, zero-quantum coherence, and second order coupling are negligible, it is possible to measure J to a precision of $\pm$N for a digitisation of N Hz/point.

Because cross-peaks are in-phase, overlap adds and can easily be reduced by applying severe resolution enhancement without affecting the measured J. One dimensional spectral simulation of cross-sections showed that after resolution enhancement, error in the measured J due to overlap is minimal. In the case of the H6/H6′ correlation, care must be taken to ensure that contributions from zero-quantum coherence are negligible. It is expected that at a 500 ms mixing time all of the zero-quantum should be relaxed, and this is confirmed by the good agreement of the J's measured from the H6/H6′ correlation with those obtained from the H6/H6′ cross-peaks, where there can be no zero-quantum contribution. Although second order coupling will not affect the measured J in a two spin system, the same is not true for larger spin systems. The H5, H6, and H6′ can be considered as an ABX spin system with H6′ as the X part. The X part of an ABX spin system is comprised of six lines, four X transitions and two M transitions. The theoretical analysis of such an ABX system (Corio 1966) using the measured chemical shifts and

Table 1. The major oligomannose oligosaccharides from bovine thyroglobulin and the variant surface glycoprotein of *T. brucei*. Percentages in brackets refer to the molar proportion of each isomer of the parent structure

$Man_9GlcNAc_2$	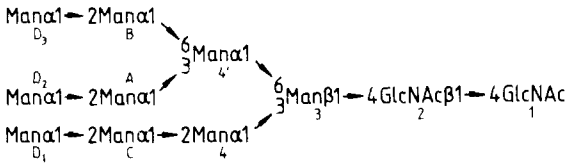	M9: BTG(100%), VSG(100%)
$Man_8GlcNAc_2$	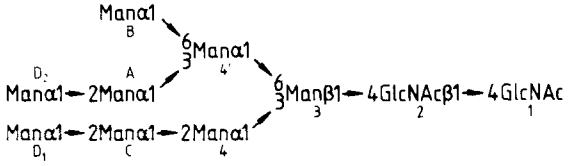	M8(D1,D2): BTG(30%), VSG(0%)
	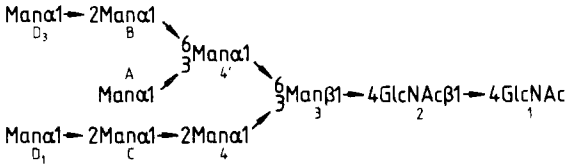	M8(D1,D3): BTG(60%), VSG(50%)
	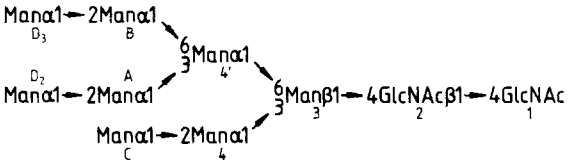	M8(D2,D3): BTG(10%), VSG(50%)
$Man_7GlcNAc_2$	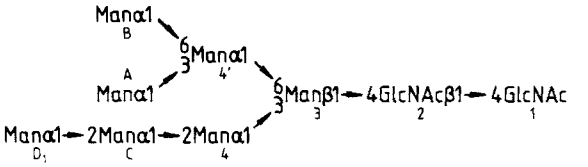	M7(D1): BTG(~100%), VSG(~0%)
	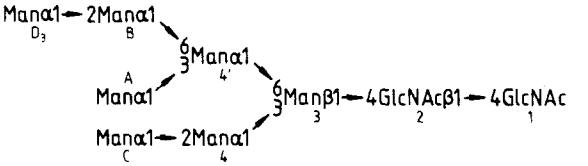	M7(D3): BTG(~0%), VSG(~100%)
$Man_6GlcNAc_2$	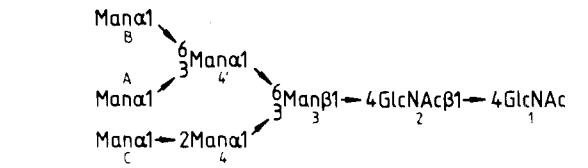	M6: BTG(~100%), VSG(~100%)
$Man_5GlcNAc_2$	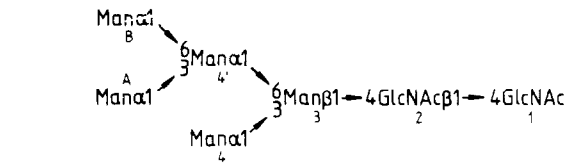	M5: BTG(100%)

coupling constants shows that the error due to strong coupling will certaintly be less than 0.1 Hz.

Cross-sections through the H6/H6′ correlations for residues 3 and 4′ of $Man_9GlcNAc_2$ and $Man_5GlcNAc_2$ are shown in Fig. 3. While $J_{5\,6'}$ can be easily measured, $J_{5\,6}$ is too small to be resolved. An upper limit can be placed on $J_{5\,6}$ by noting that the coupling becomes unresolvable when $v_{1/2} = 1.4$ J. Careful shimming and measuring linewidths of several different lines gave values at about 4.4 Hz, yielding a maximum $J = v_{1/2}/1.4 = 3.1$ Hz. To obtain a lower limit on $J_{5\,6'}$ we take the minimum value of $J_{5\,6}$ predicted by the Altona-Haasnoot parametrisation of the Karplus equation (Haasnoot et al. 1980). The chemical shifts for H5, H6, H6′ together with $J_{5\,6}$ and $J_{5\,6'}$ for residues 3 and 4′ of $Man_9GlcNAc_2$ and $Man_5GlcNAc_2$ are given in Table 2. We note that we have refined the values of our previous study. (Homans et al. 1986).

For the remaining oligomannose structures, measuring the J's from the H6/H6′ correlation can be difficult or

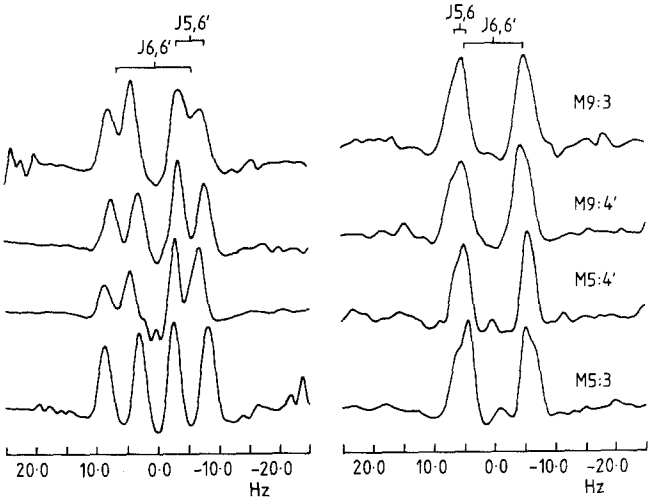

Fig. 3. NOESY cross-sections through the H6/H6′ correlation for residues 3 and 4′ of $Man_9GlcNAc_2$ (M9) (left) and $Man_5GlcNAc_2$ (M5) (right). The coupling constants $J_{5\,6}$, $J_{5\,6'}$, and $J_{6\,6'}$ are shown

impossible because of cross-peak overlap of different isomers or poor signal-to-noise ratios, and here the measurement must be made using the NOE's from H1 to H6 and H6′. In this case the $J_{5\,6'}$ can also be impossible to measure precisely because of the fact that the H1 to H6′ NOE is small. In the case of the BH1 to 4′H6′ NOE, the 4′H6′ proton is partially or fully obscured by the BH1/BH2 cross-peak. These situations are shown in Fig. 4. Figure 4A shows cross-sections through the NOESY spectrum at 4′H1 giving the NOE's to 3H6 and 3H6′. As all isomers of a given oligomannose structure possess residue 4′, and all have closely magnetically equivalent environments, cross-peaks corresponding to all structures will be present. Assignments of these cross-peaks for mixtures are then made by assuming that all isomers have the same effective correlation time, and hence the relative intensities of the H6 cross-peaks are a reflection of the relative amounts of isomers as determined from the 1-D spectrum.

Figure 4B and C shows cross-sections through BH1. Note that, unlike the 4′H1 case, there are two BH1's to consider as BH1 resonates at different frequencies de-

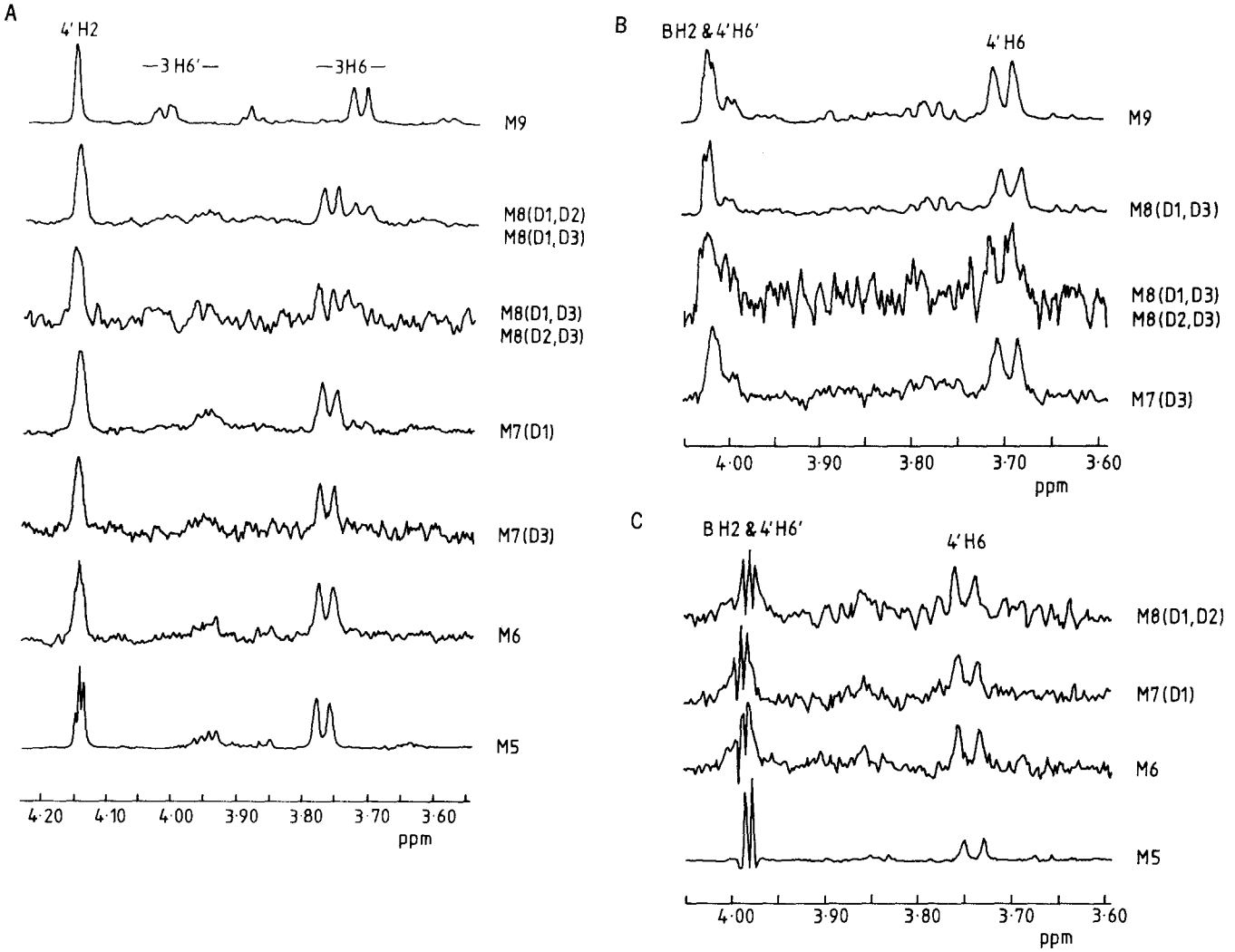

Fig. 4A–C. Cross-sections through NOESY spectra of the oligomannose oligosaccharides from BTG and VSG at **A** 4′H1, **B** BH1 when substituted by D3, and **C** BH1 when unsubstituted

Table 2. Assignments (ppm) and coupling constants (Hz) for the H5, H6 and H6′ protons of residues 3 and 4′ of $Man_9GlcNAc_2$ and $Man_5GlcNAc_2$

	M9 : 3	M9 : 4′	M5 : 3	M5 : 4′
H5	3.58	3.80	3.62	3.80
H6	3.72	3.70	3.77	3.74
H6′	4.02	4.00	3.95	3.98
$J_{5\,6}$	2.2±0.9	2.2±0.9	2.2±0.9	2.2±0.9
$J_{5\,6'}$	3.4±0.3	4.3±0.3	5.5±0.3	4.1±0.3

Table 3. Rotamer populations (%) about the C5–C6 bond of residues 3 and 4′ of the oligomannose oligosaccharides from bovine thyroglobulin and the variant surface glycoprotein of *T. brucei*

	P_{180} (±7)	P_{-60} (±6)	P_{60} (±9)
3A[a]			
M9 : 3	80	25	−5
M9 : 4′	71	39	−10
M8 (D1, D2) : 3	80	25	−5
M8 (D1, D2) : 4′	73	37	−10
M8 (D1, D3) : 3	59	41	0
M8 (D1, D3) : 4′	71	39	−10
M8 (D2, D3) : 3	80	25	−5
M8 (D2, D3) : 4′	71	39	−10
M7 (D1) : 3	59	41	0
M7 (D1) : 4′	73	37	−10
M7 (D3) : 3	59	41	0
M7 (D4) : 4′	71	39	−10
M6 : 3	59	41	0
M6 : 4′	73	37	−10
M5 : 3	59	41	0
M5 : 4′	73	37	−10
	P_{180} (±6)	P_{-60} (±5)	P_{60} (±8)
3B[b]			
M9 : 3	76	18	6
M9 : 4′	68	27	5
M8 (D1, D2) : 3	76	18	6
M8 (D1, D2) : 4′	70	25	5
M8 (D1, D3) : 3	57	40	3
M8 (D1, D3) : 4′	68	27	5
M8 (D2, D3) : 3	76	18	6
M8 (D2, D3) : 4′	68	27	5
M7 (D1) : 3	57	40	3
M7 (D1) : 4′	70	25	5
M7 (D3) : 3	57	40	3
M7 (D3) : 4′	68	27	5
M6 : 3	57	40	3
M6 : 4′	70	25	5
M5 : 3	57	40	3
M5 : 4′	70	25	5

[a] Calculated from the equation of Haasnoot et al. 1980
[b] Calculated from the equation of Wu et al. 1983

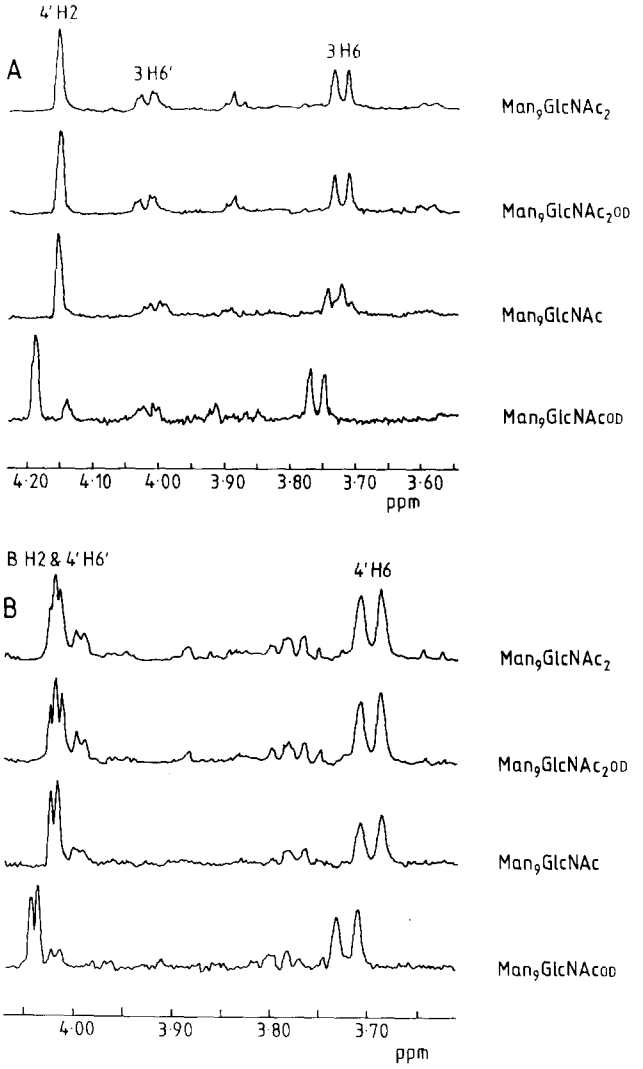

Fig. 5A, B. NOESY cross-sections through **A** 4′H1 and **B** BH1 of $Man_9GlcNAc_2$ when the structure is unreduced, reduced, treated with Endo-H, or reduced following Endo-H treatment

pending on whether it is substituted by residue D3. In the case where B is unsubstituted, it is impossible to measure $J_{5\,6'}$ since 4′H6′ lies under BH2. A very important point, however, is that in all cases, H6 is clearly resolved, and the position of the H6 resonance will change as a function of the rotamers present; for example, O4 will deshield H6 when $\omega = -60°$ (Fig. 2). The chemical shift of H6 (and H6′) is thus potentially sensitive to ω in the same way as J and so the chemical shift can be used to infer the values of $J_{5\,6}$ and $J_{5\,6'}$. It can be dangerous to rely on chemical shift data alone; however, the subspectra in Fig. 4 show remarkable consistency in the chemical shifts throughout the oligomannose series, and hence inferring J from the chemical shift in order to get ω seems valid.

It is seen that for residue 3, H6 can resonate at 3.77 ppm with $J_{5\,6}$ of 2.2 Hz as in $Man_5GlcNAc_2$ or at 3.72 ppm with $J_{5\,6}$ of 2.2 Hz as in $Man_9GlcNAc_2$. H6′ comes at either 3.95 ppm and $J_{5\,6'}$ equalling 5.5 Hz as in $Man_5GlcNAc_2$ or 4.02 ppm and $J_{5\,6'}$ of 3.4 Hz as in $Man_9GlcNAc_2$. Similarly 4′H6 can resonate at 3.74 ppm or 3.70 ppm both with $J_{5\,6'}$'s of 2.2 Hz in $Man_5GlcNAc_2$ and $Man_9GlcNAc_2$ respectively. 4′H6′ can occur at 3.98 ppm or 4.00 ppm with effectively the same $J_{5\,6'}$, 4.1 Hz for $Man_5GlcNAc_2$ and 4.3 Hz for $Man_9GlcNAc_2$.

The most striking observations to be made from Fig. 4 are the conditions under which the H6's change their resonance position. Careful examination reveals that when residue D2 is present, the H6 of residue 3 is

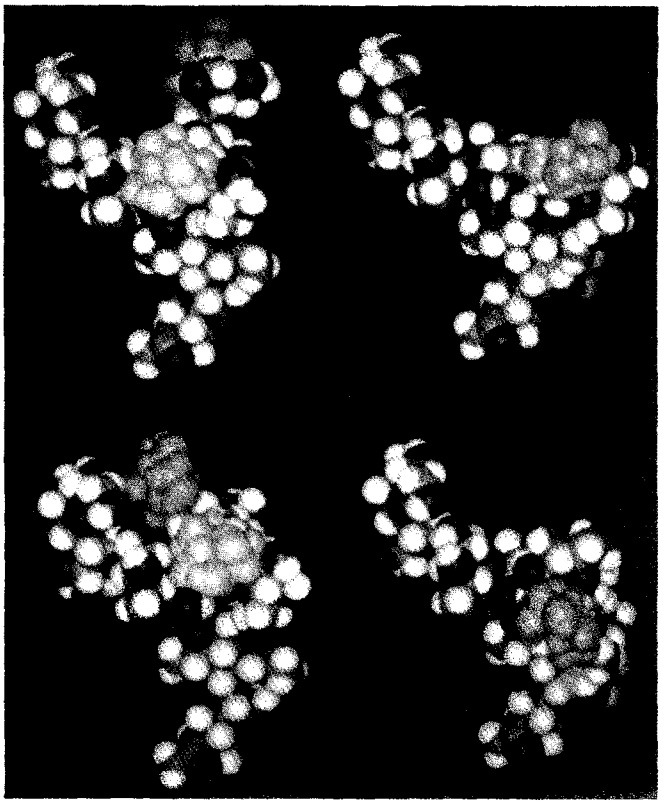

Fig. 6. The $Man_9GlcNAc_2$ structure, derived from NOE constraints and AMBER minimisation, is shown in the four possible conformations (ω(Manα1–6Manβ), ω(Manα1–6Manα)) of (clockwise from top left) A (180°, 180°), B (−60°, 180°), C (180°, −60°), and D (−60°, −60°). Residue D2 is shown in yellow and residue D3 is shown in red. There is an unfavorable steric interaction between residue D2 and GlcNAc1 and GlcNAc2 in B and D. There also may be a small unfavorable steric interaction between residue D3 and GlcNAc2 in D

found at 3.72 ppm, but upon removal of this residue H6 becomes deshielded to 3.77 ppm. In the case of residue 4′, when D3 is present H6 resonates at 3.70 ppm, but becomes deshielded to 3.74 ppm when D3 is absent. In the former case, this chemical shift difference implies a shift from $J_{5\,6'} = 3.4$ Hz to $J_{5\,6'}$ 5.5 Hz upon removal of D2. In the latter case, the coupling constants stay effectively the same, although as will be discussed, the chemical shift may be used independently to make arguments about the conformation.

Several Karplus relationships have been proposed, but there has been little improvement upon the widely used equations of either Wu et al. (1983) or of Haasnoot et al. (1980). Calculated values of rotamer populations using this last method and both equations are shown in Table 3. The uncertainties in the populations come from propagation of uncertainties in J only, and no attempt has been made to address uncertainty in the J values calculated from the Karplus equation.

Figure 5 shows NOESY cross-sections through 4′H1 and BH1 for $Man_9GlcNAc_2$ when the structure is reduced, treated with Endo-H, or reduced subsequent to Endo-H treatment. Figure 6A–D shows the $Man_9GlcNAc_2$ structure, derived from NOE constraints and AMBER minimisation, in the four possible conformations (ω(Manα1–6Manβ), ω(Manα1–6Manα)) of (180°, 180°), (−60°, 180°), (180°, −60°), and (−60°, −60°).

Discussion

The results presented here clearly show that there is variation in conformation within the oligomannose series and that this variation depends upon primary sequence. Because of the crudeness of the three state model, only a qualitative picture of the conformations of these compounds can be obtained at this stage from the NMR data. A more detailed picture would clearly involve considering distributions of rotamers about different potential wells, rather than the fixed rotamers implied by our model. Different approaches have been used. Cumming and Carver (1987) used HSEA based calculations to obtain ensemble averaged J's. Homans et al. (1986) used molecular orbital calculations to derive stable energy minima and then fitted those to measured J's. However, these approaches do not provide more accurate results given the inherent uncertainties in the theoretical models, Karplus equation, and experimental data. In fact, while the qualitative picture can reliably be derived from NMR, the detailed picture must necessarily depend for the most part on theoretical energy calculations and molecular dynamics simulations including solvent. Reliable calculations are only now becoming available on model compounds (Edge et al. 1990). The results obtained from the classical three state approach are summarised below.

In all cases, it is seen that the $\omega = +60°$ conformer is not significantly populated. This result is in agreement with many experimental and theoretical studies (Marchessault and Perez 1979; Ohrui et al. 1985; Homans et al. 1986; Berman 1987; Nishida et al. 1988), and has been explained by invoking the Hassel-Ottar effect (Hassel and Ottar 1947), a syn-periplanar repulsion between O4 and O6 that can significantly destabilise the $\omega = +60°$ form. The negative values (Table 3) for P_{60} have recently been shown to stem from imperfect staggering of the three conformers (Nishida et al. 1988). The rotamers in solution will thus be distributed between the remaining two dihedral angles, and the degree to which P_{180} and P_{-60} are the same is a measure of the dynamic flexibility of the linkage.

It is seen that the Manα1–6Manβ (4′ to 3) linkage possesses a high degree of flexibility when residue D2 is absent ($P_{-60}/P_{180} \approx 40/60$), but upon addition of this residue, flexibility becomes low with a preference for $\omega = 180°$ ($P_{-60}/P_{180} \approx 20/80$). The Man$\alpha$1–6Man$\alpha$ (B to 4′) linkage shows a flexibility which is intermediate between the two Manα1–6Manβ extremes and is largely invariant to changes in primary sequence ($P_{-60}/P_{180} \approx$ 30/70). Since the 4′H6 resonance moves downfield upon addition of D3, it may be argued that removal of D3 shifts the equilibrium slightly toward $\omega = -60$. (The H6 resonance is expected to be more deshielded with increasing population of $\omega = -60$, because H6 is brought close to O4 in this conformer.)

These observations may be rationalised by considering the AMBER minimised structure of $Man_9GlcNAc_2$ in the various conformations (ω(Manα1-6Manβ), ω(Manα1-6Manα)) seen in Fig. 6 A–D. It is observed that when $Man_9GlcNAc_2$ is in the (180°, 180°) conformation, the arms and core are spread apart and do not interact significantly with each other. In the (−60°, 180°) conformation, however, residue D2 makes Van der Waals contact with the terminal GlcNAc1 and to a lesser extent with GlcNAc2. It is therefore expected that in the presence of residue D2, the $\omega = -60°$ state of the Manα1-6Manβ linkage would be so high in energy as to have a small population.

The above conclusions regarding residue D2 provide a firm molecular basis to observations made as early as 1980 (Cohen and Ballou 1980) that in oligomannose oligosaccharides which had been treated with Endo-H (an enzyme which cleaves between the two GlcNAc's of the core thereby leaving GlcNAc2 as the reducing terminus) the H1 of residue A was split into two. In their study of $Man_9GlcNAc$, van Halbeek et al. (1980) suggested that this split at 5.398/5.409 ppm derives from the "anomerization effect", where the H1 senses the anomericity of the terminal GlcNAc. Because the effect is so much smaller in the other residues, they argued, it must indicate that residue A is close to GlcNAc2, and so the A-D2 branch of $Man_9GlcNAc_2$ must be oriented along the core. In their comparison of $Man_9GlcNAc$ and $Man_8GlcNAc$, where the major isomer lacked D2, Byrd et al. (1982) noted that whereas the split resonance of $Man_9GlcNAc$ occurs at 5.397/5.409 with a difference of 0.010 ppm, the same split in $Man_8GlcNAc$ occurs at 5.106/5.071 with a difference of 0.035 ppm. They interpreted this as showing that the interaction in $Man_8GlcNAc$ was fundamentally different from the one discussed by van Halbeek et al. (1980).

It is, though, the same interaction, for as van Halbeek et al. (1980) at least imply, the strength of the interaction, and hence the magnitude of the splitting, will depend upon the proximity of AH1 to the anomeric center. In the case of structures with D2, the splitting will be small (0.010 ppm) because the conformation which places residue A close to the reducing terminus is sterically hindered by D2. Conversely, structures without D2 will show a large (0.035 ppm) splitting because A spends a large part (40%) of its time next to GlcNAc2. The reducing terminus of $Man_9GlcNAc_2$ was reduced with sodium borodeuteride. No change in rotamer distribution was observed. The chain was then cleaved with Endo-H to give $Man_9GlcNAc$. Although a slight increase in $J_{5\,6'}$ does occur, no gross change in conformation is observed, thereby formally proving that the observations and interpretations made regarding the anomerization effect are not completely artifactual.

By contrast with D2, the effect of D3 is not easily rationalised. Although chemical shifts suggest that loss of D3 may confer additional flexibility on the Manα1-6Manα linkage, examination of the conformers (180°, 180°) and (180°, −60°) of the AMBER minimised structure for $Man_9GlcNAc_2$ (Fig. 6) does not show any reason why either should be higher in energy with or without D3. There is also no obvious indication of why the flexibility of this linkage should be intermediate between the extremes of the other linkage. Another point to consider is the mutual exclusivity of the four conformational states (180°, 180°), (180°, −60°), (−60°, 180°), and (−60°, −60°). In other words, it may not be possible to achieve all four states independently. The first two conformations should be invariant to primary sequence, while the second two should have reduced populations with D2. In addition, however, Fig. 6 shows that D3 may sterically hinder the (−60°, −60°) conformation because there is a small unfavorable steric interaction between D3 and the core.

In the first instance, conformational transitions in oligomannose oligosaccharides are governed by a conformational selection rule which allows transitions only between the $\omega = 180°$ and $\omega = -60°$ states. The physical basis for this rule lies in an unfavorable syn-periplanar interaction (Hassel-Ottar effect). Other transitions may additionally be forbidden with the presence of certain residues. These further selection rules have their basis in steric hindrance caused by interactions between distal residues.

Although rotamer populations determined by Karplus relationships may only be viewed qualitatively, we may still speculate on the possible biological role of these conformational transitions. Oligomannose oligosaccharides are intermediates common to the N-linked oligosaccharide biosynthetic pathways of both plants and animals. The work of Schachter (Schachter et al. 1983; Schachter 1986) has suggested that in addition to the relative activities of pathway enzymes, biosynthetic outcome can be controlled by the addition or removal of key residues which convert substrates into non-substrates and vice versa, leading to the proposal that N-linked oligosaccharide biosynthesis can be either sterically (Brisson and Carver 1983d) or conformationally (Homans et al. 1987a) controlled.

The results obtained in the present study are consistent with a conformationally driven biosynthetic model. It appears that the major structure to leave the rough endoplasmic reticulum (RER) is the $Man_8GlcNAc_2$ isomer without D2, unless there is a delay, in which case $Man_6GlcNAc_2$ is the major structure (Kornfeld and Kornfeld 1985). Lubas and Spiro (1988) have recently provided evidence that there are two possible processing pathways. One pathway retains residue D2, while the other tends to lose D2. It is therefore possible that a transport receptor in the RER lumen will recognise the $\omega = -60°$ conformer, but not the $\omega = 180°$ conformer. Hence, proteins with $Man_8GlcNAc_2$ having a high proportion of $\omega = -60°$ would be transported to the *cis*-Golgi, whereas those with $Man_9GlcNAc_2$ would not.

It is also possible to conceive of biological systems with two kinds of receptor, one for the $\omega = 180°$ conformer and another for the $\omega = -60°$ form. Although structures without D2 could still be recognised by the $\omega = 180°$ receptor, the rate of recognition/transport might be very much less than that for structures with D2 (in which the 180° conformer is more populated), if the rate of interconversion between the two rotamers was very much greater than the timescale for recognition. Evidence

for such conformational modulation of reaction kinetics can be seen by following the digestion products as a function of time of oligomannose structures treated with jack bean α-mannosidase (Maley and Trimble 1981; Berman and Allerhand 1981; Carver and Brisson 1984). As might be expected in light of the above discussion, it is found that the Manα1–3Manβ linkage is cleaved much more rapidly than the Manα1–3Manα linkage, the linkage on the 1–6 arm.

We note the evidence recently provided by Lazzarino and Gabel (1989) that the sequence of mannose processing and resulting conformational changes are an important factor in the phosphorylation patterns of the oligomannose oligosaccharides of acid hydrolases.

Acknowledgements. The Glycobiology Unit is supported by Monsanto. E. W. W. thanks the Rhodes Scholarship Trust for financial support.

References

Altona C, Haasnoot CAG (1980) Prediction of anti and gauche vicinal proton-proton coupling constants in carbohydrates: a simple additivity rule for pyranose rings. Org Magn Res 13:417–429

Ashford D, Dwek RA, Welply JK, Amatayakul S, Homans SW, Lis H, Taylor GN, Sharon N, Rademacher TW (1987) The β1-2-D-Xylose and α1-3-L-Fucose substituted N-linked oligosaccharides from *Erythrina cristagalli* lectin. Isolation, characterization and comparison with other legume lectins. Eur J Biochem 166:311–320

Aue WP, Bartholdi E, Ernst RR (1976) Two-dimensional spectroscopy. Application to nuclear magnetic resonance. J Chem Phys 64:2229–2246

Berman E (1987) Conformational analysis and the fine structure of the cross peaks in phase-sensitive homonuclear two-dimensional correlated NMR spectra of oligosaccharides. Eur J Biochem 165:385–391

Berman E, Allerhand A (1981) Kinetics of α-D-mannopyranosyl linkages in hen ovalbumin glycopeptides as monitored by carbon-13 nuclear magnetic resonance spectroscopy. J Biol Chem 256:6657–6662

Biswas M, Sekharudu YC, Rao VS (1987) The conformation of the oligo-D-mannosidic type, and their interaction with glycans of concanavalin A: a computer-modelling study. Carbohydr Res 160:151–170

Bock K, Arnap J, Lonngren J (1982) The preferred conformation of oligosaccharides derived from the complex-type carbohydrate portions of glycoproteins. Eur J Biochem 129:171–178

Brisson JR, Carver JP (1983a) Solution conformation of alpha D(1-3)- and alpha D(1-6)-linked oligomannosides using proton nuclear magnetic resonance. Biochemistry 22:1362–1368

Brisson JR, Carver JP (1983b) Solution conformation of asparagine-linked oligosaccharides: alpha(1-2)-, alpha(1-3)-beta(1-2)- and beta(1-4)-linked units. Biochemistry 22:3671–3680

Brisson JR, Carver JP (1983c) Solution conformation of asparagine-linked oligosaccharides: alpha(1-6)-linked moiety. Biochemistry 22:3680–3686

Brisson JR, Carver JP (1983d) The relation of three-dimensional structure to biosynthesis in the N-linked oligosaccharides. Can J Biochem Cell Biol 61:1067–1078

Bush CA, Yan ZY, Rao BNN (1986) Conformational energy calculations and proton nuclear Overhauser enhancements reveal a unique conformation for blood group A oligosaccharides. J Am Chem Soc 108:6168–6173

Byrd JC, Tarentino AL, Maley F, Atkinson PH, Trimble RB (1982) Glycoprotein synthesis in yeast. Identification of $Man_8GlcNAc_2$ as an essential intermediate in oligosaccharide processing. J Biol Chem 257:14657–14666

Cohen RE, Ballou CE (1980) Linkage and sequence analysis of mannose-rich glycoprotein core oligosaccharide by proton nuclear magnetic resonance spectroscopy. Biochemistry 19:4345

Corio PL (1966) Structure of high resolution NMR spectra. Academic Press, New York, pp 299–305

Cumming DA, Carver JP (1987) Virtual and solution conformations of oligosaccharides. Biochemistry 26:6664–6676

Edge CJ, Singh UC, Bazzo R, Taylor GL, Dwek RA, Rademacher TW (1990) 500 Picosecond molecular dynamics in water of the Manα → 2Manα glycosidic linkage present in Asn-linked oligomannose type structures on glycoproteins. Biochemistry 29:1971–1974

Eich G, Bodenhausen G, Ernst RR (1982) Exploring nuclear spin systems by relayed magnetization transfer. J Am Chem Soc 104:3731–3732

Haasnoot CAG, DeLeeuw FAAM, Altona C (1980) The relation between proton-proton NMR coupling constants and substituent electronegativities. An empirical generalization of the Karplus equation Tetrahedron 36:2783–2792

Hassel O, Ottar B (1947) The structure of molecules containing cyclohexane or pyranose ring. Acta Chem Scand 1:929–943

Homans SW, Dwek RA, Fernandes DL, Rademacher TW (1983a) The use of two-dimensional correlated spectroscopy to obtain new assignments in the high-resolution ^1H nuclear magnetic resonance spectrum of the biantennary complex oligosaccharide isolated from human serum transferrin by hydrazinolysis. Biochim Biophys Acta 760:256–261

Homans SW, Dwek RA, Fernandes DL, Rademacher TW (1983b) Solution conformation of biantennary complex type oligosaccharides: determination of major conformers about the glycosidic linkages. FEBS Lett 164:231–235

Homans SW, Dwek RA, Fernandes DL, Rademacher TW (1984) Multiple-step relayed correlation spectroscopy: sequential resonance assignments in oligosaccharides. Proc Natl Acad Sci 81:6286–6289

Homans SW, Dwek RA, Boyd J, Mahmoudian M, Richards WG, Rademacher TW (1986) Conformational transitions in N-linked oligosaccharides. Biochemistry 25:6342–6350

Homans SW, Dwek RA, Boyd J, Soffe N, Rademacher TW (1987a) A method for the rapid assignment of ^1H NMR spectra of oligosaccharides using homonuclear Hartmann-Hahn spectroscopy. Proc Natl Acad Sci USA 84:1202–1205

Homans SW, Dwek RA, Rademacher TW (1987b) Tertiary structure in N-linked oligosaccharides. Biochemistry 26:6553–6560

Homans SW, Pastore A, Dwek RA, Rademacher TW (1987c) Structure and dynamics in oligomannose-type oligosaccharides. Biochemistry 26:6649–6655

Homans SW, Dwek RA, Rademacher TW (1987d) Solution conformations of N-linked oligosaccharides. Biochemistry 26:6571–6578

Homans SW, Edge CJ, Ferguson MAJ, Dwek RA, Rademacher TW (1989) Solution structure of the glycosyl-phosphatidylinositol membrane anchor glycan of trypanosoma brucei variant surface glycoprotein. Biochemistry 28:2881–2887

Jeener J, Meier BH, Bachmann P, Ernst RR (1979) Investigation of exchange processes by two-dimensional NMR spectroscopy. J Chem Phys 71:4546–4553

Karplus M (1959) Contact Electron-Spin Coupling of Nuclear Magnetic Moments. J Chem Phys 30:11–15

Koerner TA, Prestegard JH, Yu RK (1987) Oligosaccharide structure by two-dimensional proton nuclear magnetic resonance spectroscopy. Methods Enzymol 138:38–59

Kornfeld R, Kornfeld S (1985) Assembly of asparagine-linked oligosaccharides. Ann Rev Biochem 54:631–664

Kumar A, Ernst RR, Wuethrich K (1980) A two-dimensional nuclear Overhauser exchange (2D NOE) experiment for the elucida-

tion of complete proton-proton cross-relaxation networks in biological macromolecules. BBRC 95:1–6

Lazzarino DA, Gabel CA (1989) Mannose processing is an important determinant in the assembly of phosphorylated high mannose-type oligosaccharides. J Biol Chem 264:5015–5023

Lemieux RU, Bock K, Delbaere LTJ, Koto S, Rao VS (1980) The conformations of oligosaccharides related to the ABH and Lewis human blood group determinants. Can J Chem 58:631–653

Lubas WA, Spiro RG (1988) Evaluation of the role of rat liver Golgi *endo*-alpha-D-mannosidase in processing N-linked oligosaccharides. J Biol Chem 263:3990–3998

Macura S, Huang Y, Suter D, Ernst RR (1981) Two-dimensional chemical exchange and cross-relaxation spectroscopy of coupled nuclear spins. J Mag Res 43:259–281

Maley F, Trimble RB (1981) Revision of the structure for an *endo*-β-N-acetylglucosaminidase H substrate using a novel modification of the Smith degradation. J Biol Chem 256:1088–1090

Marchessault RH, Perez S (1979) Conformation of the hydroxymethyl group in crystalline aldohexopyranoses. Biopolymers 18:2369–2374

Marion D, Wuthrich K (1983) Application of phase sensitive two-dimensional correlated spectroscopy (COSY) for measurements of 1H-1H spin-spin coupling constants in proteins. Biochem Biophys Res Commun 113:967–974

Nishida Y, Hori H, Ohrui H, Meguro H (1988) Proton NMR analysis for rotameric distribution of the C(5)–C(6) bonds of D-glucopyranoses in solution. J Carb Chem 7:239–250

Ohruni H, Nishida Y, Watanabe M, Hori H, Meguro H (1985) Proton-NMR studies on (6R)- and (6S)-deuterated (1–6)-linked disaccharides: assignment of the preferred rotamers about C5–C6 bond of (1–6) disaccharides in solution. Tet Lett 26:3251

Parekh RB, Tse AGC, Dwek RA, Williams AF, Rademacher TW (1987) Tissue-specific N-glycosylation, site-specific oligosaccharide patterns and lentil lectin recognition of rat Thy-1. EMBO J 6:1233–1244

Paulsen H, Peters T, Sinnwell V, Heume M, Meyer B (1986) Conformational analysis of the double pentasaccharide sequence of the "bisected" structure of N-glycoproteins. Carbohydr Res 156:87–106

Rademacher TW, Parekh RB, Dwek RA (1988) Glycobiology. Ann Rev Biochem 57:785–838

Schachter H (1986) Biosynthetic controls that determine the branching and microheterogeneity of protein-bound oligosaccharides. Adv Exp Med Biol 205:53–85

Schachter H, Narasimhan S, Gleeson P, Vella G (1983) Glycosyltransferases involved in elongation of N-glycosidically linked oligosaccharides of the complex or N-acetyllactosamine type. Methods Enzymol 98:98–134

Van Halbeek H, Dorland L, Veldink GA, Vliegenthart JFG, Streker G, Michalski JC, Montreuil J, Hull WE (1980) A 500 MHz proton NMR study of urinary oligosaccharides from patients with mannosidosis. FEBS Lett 121:71–77

Vliegenthart JFG, Dorland L, Van Halbeek H (1983) High-resolution, H-nuclear magnetic resonance spectroscopy as a tool in the structural analysis of carbohydrates related to glycoproteins. Adv Carbohydr Chem Biochem 41:209–374

Wu GD, Serrianni AS, Barker R (1983) Stereoselective deuterium exchange of methylene protons in methyl tetrafuranosides: hydroxymethyl group conformations in methyl pentafuranosides. J Org Chem 48:1750–1757

Yan ZY, Rao BNN, Bush CA (1987) Influence of non-aqueous solvents on the conformation of blood group oligosaccharides. J Am Chem Soc 109:7663–7669

Zamze SE, Wooten WE, Ashford DA, Ferguson MAG, Dwek RA, Rademacher TW (1990) Characterisation of the asparagine-linked oligosaccharides from *Trypanosoma brucei* type I variant surface glycoproteins. Eur J Biochem 187:657–663